Isospin violating decay $D_s^* \to D_s\pi^0$ in chiral perturbation theory

Bin Yang,[1,*] Bo Wang,[2,1,†] Lu Meng,[1,‡] and Shi-Lin Zhu[1,2,§]

[1]*School of Physics and State Key Laboratory of Nuclear Physics and Technology, Peking University, Beijing 100871, China*

[2]*Center of High Energy Physics, Peking University, Beijing 100871, China*

(Received 29 December 2019; accepted 28 February 2020; published 16 March 2020)

We systematically calculate the isospin violating decay, $D_s^* \to D_s\pi^0$, with heavy meson chiral perturbation theory up to $\mathcal{O}(p^3)$ including the loop diagrams. The $\mathcal{O}(p^3)$ tree-level amplitudes contain four undetermined low energy constants. We use two strategies to estimate them. Using the nonanalytic dominance approximation, we get $\Gamma[D_s^* \to D_s\pi^0] = 8.1^{+3.0}_{-2.6}$ eV. Using the naturalness assumption, we obtain the range of the isospin violating decay width as [5.2, 11.7] eV. These two strategies give similar sizes. We find that the contribution of the $\mathcal{O}(p^3)$ corrections might be significant.

DOI: 10.1103/PhysRevD.101.054019

I. INTRODUCTION

The $D_{(s)}$ mesons are composed of one charm quark and one light antiquark. The dynamics of $D_{(s)}$ mesons is constrained by both the chiral symmetry in the light quark sector and the heavy quark symmetry in the heavy sector. The subtle interplay of the light and heavy degrees of freedom within the $D_{(s)}$ mesons renders them a crucial platform to explore and understand QCD. Note that $D_{s0}^*(2317)$ and $D_{s1}(2460)$ are two superstars in the D_s family due to their unexpected low mass [1,2]. The coupled-channel effect between the $DK^{(*)}$ scattering states and $c\bar{s}$ components leads to the mass deviation from the quark model prediction [3–5]. See Ref. [6] for a recent review. In addition, the charm quark mass is not very large. Thus, decay behaviors of $D_{(s)}$ mesons will provide us with very important information about the heavy quark symmetry and the light quark dynamics.

The strong and radiative decays of the charmed mesons have been studied in many different models. For example, chiral perturbation theory and heavy quark effective theory are used in Refs. [2,7–15]. Various quark models are employed in Refs. [1,16–22]. There are also many other theoretical methods such as the vector meson dominance hypothesis [23], QCD sum rules [24–28], quark-potential models [16,29–31], the extended Nambu-Jona-Lasinio model [32,33], the cloudy bag model [34], the constituent quark-meson model [35], lattice QCD simulations [36], and so on.

For the ground states, the mass splittings between $D_{(s)}^*$ and $D_{(s)}$ lie above the pion mass m_π with 2–3 MeV. The constraint from phase space leads to the dominant pion and photon emission decay modes of $D_{(s)}^*$, i.e., $D_{(s)}^* \to D_{(s)}\gamma$ and $D_{(s)}^* \to D_{(s)}\pi$. For the charmed strange meson D_s^*, the decay modes are particularly interesting. Note that $D_s^* \to D_s\pi^0$ is the strong decay process which violates the isospin symmetry. The double suppressions from phase space and the isospin violation make the hadron decay width tiny, at the order of several eVs. The branching ratio of this strong decay mode is $(5.8 \pm 0.7)\%$, which is much less than that of the electromagnetic decay $D_s^* \to D_s\gamma$, about $(93.5 \pm 0.7)\%$ [37]. The decay mode challenges our physical intuition about the magnitude of strong decay.

The decay ratio of $\Gamma(D_s^{*+} \to D_s^+ + \pi^0)/\Gamma(D_s^{*+} \to D_s^+ + \gamma)$ has been measured in by CLEO [38] and *BABAR* [39], respectively. Theoretically, this decay channel has been studied in Refs. [40–42] with chiral symmetry and heavy quark symmetry, where only the tree-level contributions are considered. The very exotic hadronic decay mode deserves a more refined investigation.

Chiral perturbation theory is the effective field theory of low energy QCD, which is a systematic and model-independent framework. It is a powerful tool to analyze the physics associated with the light degrees of freedom within the $D_{(s)}$ mesons below the typical energy scale, m_ρ. For the $D_{(s)}$ mesons, the charm quark mass m_c is much larger than the light quark mass $m_q (q = u, d, s)$; thus, m_c can be integrated out at the low energy scale. The color-magnetic interaction in the QCD Hamiltonian is suppressed

*bin_yang@pku.edu.cn
†bo-wang@pku.edu.cn
‡lmeng@pku.edu.cn
§zhusl@pku.edu.cn

by $1/m_c$ and can be omitted at the leading order of the heavy quark effective theory. Thus, the heavy quark is regarded as the static color source, and the heavy quark spin symmetry is kept.

In Refs. [7–9,43–46], the chiral effective theory incorporating heavy quark symmetry was constructed. In the effective theory, the chiral Lagrangian describes the low energy strong interactions between the heavy hadrons and light Goldstone bosons. Naturally, we can exploit this chiral effective theory to describe the strong decay of $D^*_{(s)} \to D_{(s)}\pi$.

In this work, we focus on the isospin violating decay $D_s^* \to D_s\pi^0$. We use heavy meson chiral perturbation theory to investigate this process. Based on previous work, we not only calculate the leading order contribution but also include the next-to-leading order loop diagrams and tree diagrams. The contributions of the loop diagrams manifest the complicated light quark dynamics, which generates some different structures from the leading ones. In addition, the m_π-dependent analytic expressions might be useful for the extrapolations in lattice QCD simulations.

This paper is organized as follows. In Sec. II, we give the effective Lagrangians with respect to the charmed mesons and light pseudoscalars. In Sec. III, we illustrate the Feynman diagrams of the decay $D_s^* \to D_s\pi^0$, the corresponding analytic expression of each diagram, and the numerical results, respectively. In Sec. IV, we give some discussions and conclusions.

II. EFFECTIVE LAGRANGIANS

One may use chiral symmetry and heavy quark symmetry to construct the Lagrangians that account for the heavy mesons and light pseudoscalars. The light pseudoscalar meson octets are described by the field $U(x) = u^2 = e^{i\phi/f_\phi}$ with

$$\phi = \begin{pmatrix} \pi^0 + \frac{1}{\sqrt{3}}\eta & \sqrt{2}\pi^+ & \sqrt{2}K^+ \\ \sqrt{2}\pi^- & -\pi^0 + \frac{1}{\sqrt{3}}\eta & \sqrt{2}K^0 \\ \sqrt{2}K^- & \sqrt{2}\bar{K}^0 & -\frac{2}{\sqrt{3}}\eta \end{pmatrix}, \tag{1}$$

and f_ϕ is the decay constant of the light pseudoscalars. Their experimental values are $f_\pi = 92.4$ MeV, $f_K = 113$ MeV, and $f_\eta = 116$ MeV, respectively. The chiral connection is defined as

$$\Gamma_\mu \equiv \frac{1}{2}(u^\dagger\partial_\mu u + u\partial_\mu u^\dagger). \tag{2}$$

The leading order Lagrangian that describes the self-interaction of the octet pseudoscalars can be written as [40,47]

$$\mathcal{L}_{\phi\phi} = \frac{f_\phi^2}{4}\mathrm{Tr}[\partial_\mu U\partial^\mu U^\dagger] + \frac{f_\phi^2}{4}\mathrm{Tr}[\chi U^\dagger + U\chi^\dagger], \tag{3}$$

where $\mathrm{Tr}[\ldots]$ denotes the trace in flavor space. The building block $\chi = 2B_0 m_q$ contains the light quark mass matrix m_q,

$$m_q = \begin{pmatrix} m_u & 0 & 0 \\ 0 & m_d & 0 \\ 0 & 0 & m_s \end{pmatrix}, \tag{4}$$

and $B_0 = -\langle\bar{q}q\rangle/(3f_\phi^2)$ is a parameter related to the quark condensate. The second term in Eq. (3) embodies the chiral symmetry breaking effect, which implies the π^0 and η mixing vertex, i.e.,

$$\mathcal{L}_{\mathrm{mixing}} = -\frac{B_0}{\sqrt{3}}(m_u - m_d)\eta\pi^0. \tag{5}$$

This equation demonstrates the origin of the isospin symmetry violation at the quark level, i.e., the tiny mass difference between u and d quarks.

The spin doublet of the anticharmed vectors $\bar{D}^*$ and pseudoscalars $\bar{D}$ can be expressed as the four-velocity dependent superfield $\mathcal{H}$ in the heavy quark limit, i.e.,

$$\begin{aligned} \mathcal{H} &= [P^*_\alpha\gamma^\alpha + iP\gamma_5]\frac{(1-\not{v})}{2}, \\ \bar{\mathcal{H}} &= \gamma_0\mathcal{H}^\dagger\gamma_0 = \frac{1-\not{v}}{2}[P^{*\dagger}_\alpha\gamma^\alpha + iP^\dagger\gamma_5], \end{aligned} \tag{6}$$

where $v = (1, \mathbf{0})$ is the four-velocity of the heavy mesons, and the charmed meson fields are denoted as

$$P^{(*)} = (\bar{D}^{0(*)}, D^{(*)-}, D_s^{(*)-}). \tag{7}$$

The leading order Lagrangian describing the low energy interactions of the anticharmed mesons and light pseudoscalars reads

$$\mathcal{L}^{(1)}_{P^*P\phi} = -i\langle\bar{\mathcal{H}}v\cdot\mathcal{D}\mathcal{H}\rangle - \frac{\Delta}{8}\langle\bar{\mathcal{H}}\sigma^{\mu\nu}\mathcal{H}\sigma_{\mu\nu}\rangle + g\langle\bar{\mathcal{H}}\not{u}\gamma_5\mathcal{H}\rangle, \tag{8}$$

where $\mathcal{D}_\mu = \partial_\mu + \Gamma_\mu$, and $\langle\ldots\rangle$ denotes the trace in spinor space. Here, $\Delta = m_{P^*} - m_P$ is the mass splitting between $\bar{D}^*$ and $\bar{D}$, and $g \approx 0.59$ represents the axial coupling constant, which can be determined from the partial decay width of $D^{*+} \to D^0\pi^+$ [15,37] or lattice QCD [48]. Note that u_μ is the chiral axial-vector current, which reads

$$u_\mu \equiv \frac{i}{2}(u^\dagger\partial_\mu u - u\partial_\mu u^\dagger). \tag{9}$$

In Eq. (8), the first term describes the kinetic energy of the heavy mesons. The second term comes from the $1/m_Q$ correction of the next-to-leading order color-magnetic interaction in the heavy quark expansion. The third term gives the coupling vertices of $\bar{D}^*\bar{D}\pi$ and $\bar{D}^*\bar{D}^*\pi$.

Next, we consider the contribution of the $\mathcal{O}(p^2)$ tree diagram. In order to construct such an $\mathcal{O}(p^2)$ Lagrangian to provide the $D_s^* D_s \pi^0$ vertex, we need the building blocks χ_- and $\partial^\mu u_\mu$. If we use the building block χ_-, one should notice that the parity of this building block is negative; i.e., we have to multiply another $\mathcal{O}(p^0)$ building block with negative parity to make sure the parity of the Lagrangian is positive. However, there does not exist such a building block that can satisfy both the requirement of parity conservation and Lorentz invariance. For the other building block $\partial^\mu u_\mu$, the same problem exists. Thus, there is no $\mathcal{O}(p^2)$ chiral Lagrangian contributing to the isospin violating process after considering the constraint from Lorentz invariance and CPT conservation.

In our calculation, we also consider the contribution from the loop diagrams, which will be presented later. According to the power counting, the chiral order of the one-loop diagrams is at least $\mathcal{O}(p^3)$. In order to absorb the divergence in the loop diagrams, the $\mathcal{O}(p^3)$ tree-level Lagrangian is constructed as follows,

$$\begin{aligned}\mathcal{L}^{(3)}_{P^*P\phi} = &\frac{b_1}{\Lambda_\chi^2}\langle \bar{\mathcal{H}} \not{v} \hat{\chi}_+ \gamma_5 \mathcal{H}\rangle + \frac{b_2}{\Lambda_\chi^2}\langle \bar{\mathcal{H}} \not{v} \gamma_5 \mathcal{H}\rangle \mathrm{Tr}[\chi_+] \\ &+ i\frac{c_1}{\Lambda_\chi^2}\langle \bar{\mathcal{H}} \not{\partial} \hat{\chi}_- \gamma_5 \mathcal{H}\rangle + \frac{d}{\Lambda_\chi^2}\langle \bar{\mathcal{H}} \partial_\nu \not{\partial} u^\nu \gamma_5 \mathcal{H}\rangle \\ &+ i\frac{c_2}{\Lambda_\chi^2}\langle \bar{\mathcal{H}} \gamma^\mu \gamma_5 \mathcal{H}\rangle \partial_\mu \mathrm{Tr}[\chi_-], \end{aligned} \tag{10}$$

where $\Lambda_\chi = 4\pi f_\pi$. Here, b_1, b_2, c_1, c_2, and d are five low energy constants (LECs). The spurions $\chi_\pm$ are introduced as

$$\chi_\pm = u^\dagger \chi u^\dagger \pm u \chi^\dagger u, \qquad \hat{\chi}_\pm = \chi_\pm - \frac{1}{3}\mathrm{Tr}[\chi_\pm]. \tag{11}$$

The Lagrangian (10) contains all possible relevant terms satisfying the requirement of the symmetries. However, the structures of the terms $\langle \bar{\mathcal{H}} \not{v} \gamma_5 \mathcal{H}\rangle \mathrm{Tr}[\chi_+]$ and $\langle \bar{\mathcal{H}} \gamma^\mu \gamma_5 \mathcal{H}\rangle \partial_\mu \mathrm{Tr}[\chi_-]$ are the same as the ones from the leading order Lagrangian. Thus, they can be absorbed into Eq. (8) by renormalizing the axial coupling g. The term $\langle \bar{\mathcal{H}} \partial_\nu \partial^\nu u_\mu \gamma^\mu \gamma_5 \mathcal{H}\rangle$ is actually the same as the fourth term in the Lagrangian in our calculation, and we did not write it in Eq. (10). With the above Lagrangians, we can analytically calculate the decay process $D_s^* \to D_s\pi^0$ up to $\mathcal{O}(p^3)$.

III. ISOSPIN VIOLATING DECAY

A. Power counting and Feynman diagrams

In chiral perturbation theory, one can use the power counting to assess the importance of Feynman diagrams generated by the effective Lagrangians when calculating the physical matrix element. The standard power counting for this process yields

$$\mathcal{O} = 4N_L - 2I_M - I_H + \sum_n n N_n, \tag{12}$$

where N_L, I_M, and I_H are the numbers of loops, internal light pseudoscalar lines, and internal heavy meson lines, respectively. Note that N_n is the number of vertices which are governed by the nth order Lagrangians. Thus, we can write the decay amplitude as the following expression,

$$\mathcal{M} = \mathcal{M}^{(1)}_{\mathrm{tree}} + \mathcal{M}^{(3)}_{\mathrm{tree}} + \mathcal{M}^{(3)}_{\mathrm{loop}}, \tag{13}$$

where the superscripts in parentheses represent the chiral order.

For the $\mathcal{O}(p)$ tree diagram, the isospin violating effect comes from the $\pi - \eta$ mixing as shown in Fig. 1. From Eq. (5), the $\pi - \eta$ mixing effect comes from the mass difference between u and d quarks.

The loop diagrams with the vertices from the leading order Lagrangians [e.g., see Eqs. (3), (8), and (10)] are shown in Fig. 2, which are $\mathcal{O}(p^3)$ diagrams according to the power counting law. The loop diagrams (k) and (l,m) are the renormalization of the D_s and D_s^* wave functions, respectively.

The vertex with two heavy mesons and one light pseudoscalar comes from the third term of the $\mathcal{O}(p)$ Lagrangian (8). The vertex denoted with the cross is from the Lagrangian (5). The vertex in the diagrams (e,f) connecting two heavy mesons and three pseudoscalars also stems from the third term of Eq. (8), where we need to expand the axial-vector field u_μ to the second order. We can derive the vertices with two heavy mesons and two light pseudoscalars in diagrams (g)–(j) from the first term of Eq. (8). The chiral connection in the covariant derivative generates this kind of vertex.

For the $\mathcal{O}(p^3)$ loop diagrams, the isospin violating effect comes from two processes. The graphs (b,d,f,h,j,k,l,m) contain the $\eta - \pi$ mixing vertex which resembles the $\mathcal{O}(p)$ tree diagram. The second type of loop diagrams (a,c,e,g,i) do not have the direct isospin violating vertex, i.e., $\eta - \pi$ mixing. The second type of isospin violation arises from incomplete cancellation of diagrams, considering the mass splitting of particles within the same isospin multiplet in the loops. For example, we consider the internal light

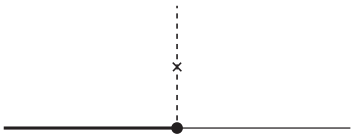

FIG. 1. The tree diagram for the $D_s^* \to D_s\pi^0$ decay at leading order. The thick solid, thin solid, and dashed lines represent the heavy vector meson D_s^*, heavy pseudoscalar meson D_s, and light pseudoscalar mesons, respectively. The solid dot denotes the $\mathcal{O}(p)$ $D_s^* D_s \eta$ vertex, and the cross represents the $\eta - \pi$ mixing vertex.

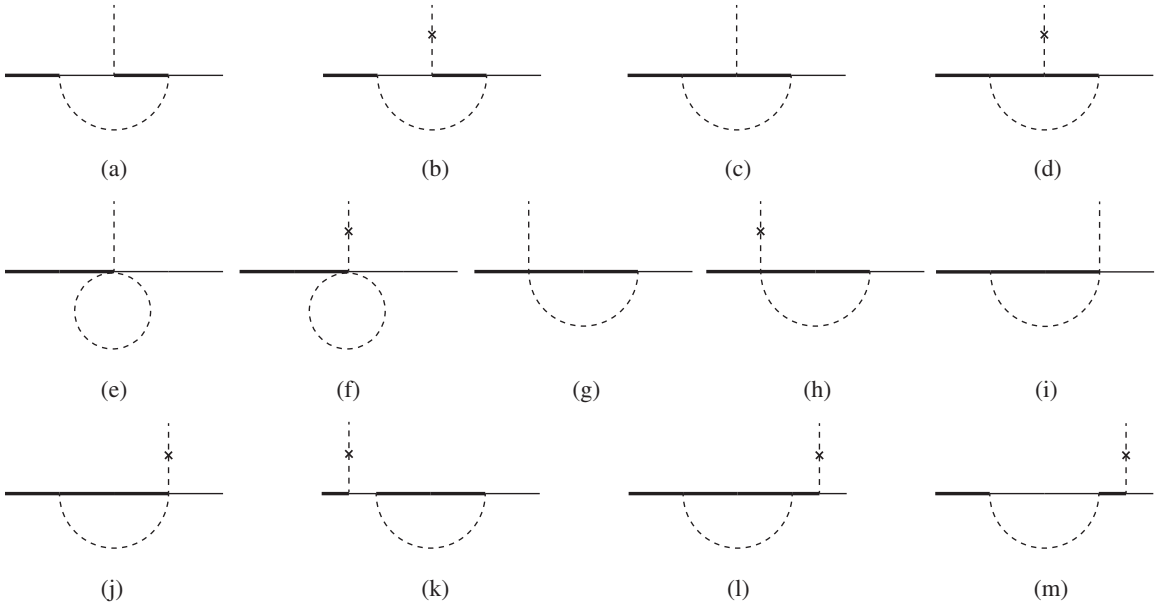

FIG. 2. The loop diagrams for the $D_s^* \to D_s\pi^0$ decay at the next-to-leading order. The notations are the same as those in Fig. 1.

pseudoscalars such as K^- and $\bar{K}^0$, when calculating the loop diagram (a). If we ignore the mass splitting between K^- and $\bar{K}^0$, their contributions are exactly the same but with opposite sign. The graph (a) becomes nonvanishing and gives the isospin violating effect when the tiny mass difference $\delta_{m_K} = m_{\bar{K}^0} - m_{K^-}$ is kept. The kaon mass difference δ_{m_K} originates from an $m_d - m_u$ difference as well as an electromagnetic effect. So, in order to avoid the influence of the electromagnetic effect as much as possible, we work directly with the $\pi^0 - \eta$ mixing angle $\theta_{\eta\pi^0}$ [see the definition in Eq. (15)] for the tree diagram and loop diagram which contain the $\pi^0 - \eta$ mixing vertex. While for the loop diagram that cannot be expressed with $\theta_{\eta\pi^0}$, we use the physical value of δ_{m_K}.

Besides the mass splitting between u and d quarks, another source of the isospin violating effect stems from the electromagnetic interaction, the charge difference between u and d quarks. The Feynman diagram is shown in Fig. 3. The vertex $\pi^0 \to 2\gamma$ denoted by the solid triangle arises from the axial-vector current anomaly. However, the Feynman amplitude of such a diagram is proportional to α^2, where α is the fine structure constant. The contribution of this diagram is highly suppressed. Thus, it is reasonable to neglect the isospin violation from the electromagnetic interaction in our calculation.

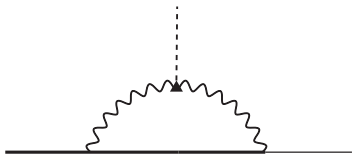

FIG. 3. A diagrammatic presentation of the axial-vector current anomaly contribution to the $D_s^* \to D_s\pi^0$ decay at the loop level. The wiggly line represents the photon, and the solid triangle denotes the $\pi^0\gamma\gamma$ coupling vertex. Other notations are the same as those in Fig. 1.

The tree diagrams with the vertices coming from the next-to-leading order Lagrangian (10) are also $\mathcal{O}(p^3)$. We show the diagrams in Fig. 4. The $\mathcal{O}(p^3)$ tree diagram can contain the $D_s^* D_s \pi^0$ vertex, which is different from the $\mathcal{O}(p)$ one.

B. Analytical results

Using Eqs. (8) and (5), one can easily get the amplitude of the $\mathcal{O}(p)$ tree diagram [see Fig. 1], which yields

$$i\mathcal{M}^{(1)} = -\frac{g}{f_\eta}(q\cdot\varepsilon)\frac{2}{\sqrt{3}}\theta_{\eta\pi^0}, \tag{14}$$

where q and ε are the momentum of π^0 and polarization vector of D_s^*, respectively. Note that $\theta_{\eta\pi^0}$ is the $\pi^0 - \eta$ mixing angle, and it is defined as

$$\theta_{\eta\pi^0} = \frac{\sqrt{3}}{4}\frac{m_d - m_u}{m_s - \hat{m}}, \tag{15}$$

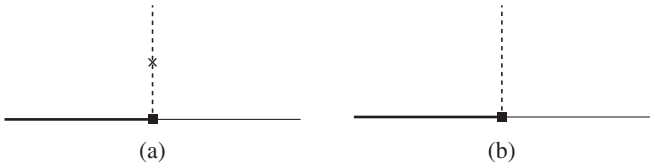

FIG. 4. The tree diagrams for the $D_s^* \to D_s\pi^0$ decay at the next-to-leading order. The solid square stands for the $\mathcal{O}(p^3)$ coupling. Other notations are the same as those in Fig. 1.

where $\hat{m} = (m_u + m_d)/2$. The values of m_u, m_d, and m_s are taken from the Particle Data Group [37].

The decay amplitudes of the $\mathcal{O}(p^3)$ loop diagrams in Fig. 2 are given as follows,

$$i\mathcal{M}^{(3)}_{(a)} = \frac{g^3}{2f_K^2 f_\pi}(q\cdot\varepsilon)\left[-\frac{F(m_{K^+},\omega_1,\delta_1)}{q_0+\Delta_1} + \frac{F(m_{K^0},\omega_2,\delta_2)}{q_0+\Delta_2}\right], \tag{16}$$

$$i\mathcal{M}^{(3)}_{(b)} = -\frac{g^3}{\sqrt{3}f_\eta}(q\cdot\varepsilon)\theta_{\eta\pi^0}\left[\frac{1}{2f_K^2}\frac{F(m_{K^+},\omega_1,\delta_1)}{q_0+\Delta_1} + \frac{1}{2f_K^2}\frac{F(m_{K^0},\omega_2,\delta_2)}{q_0+\Delta_2} - \frac{2}{3f_\eta^2}\frac{F(m_\eta,\omega_3,\delta_3)}{q_0+\Delta_3}\right], \tag{17}$$

$$i\mathcal{M}^{(3)}_{(c)} = \frac{g^3}{f_K^2 f_\pi}(q\cdot\varepsilon)\left[\frac{F(m_{K^+},\omega_1-\Delta_1,\delta_1)}{q_0} - \frac{F(m_{K^0},\omega_2-\Delta_2,\delta_2)}{q_0}\right], \tag{18}$$

$$i\mathcal{M}^{(3)}_{(d)} = -\frac{g^3(q\cdot\varepsilon)}{\sqrt{3}f_\eta}\theta_{\eta\pi^0}\left[\frac{F(m_{K^+},\omega_1-\Delta_1,\delta_1)}{-q_0 f_K^2} - \frac{F(m_{K^0},\omega_2-\Delta_2,\delta_2)}{q_0 f_K^2} + \frac{4}{3}\frac{F(m_\eta,\omega_3-\Delta_3,\delta_3)}{q_0 f_\eta^2}\right], \tag{19}$$

$$i\mathcal{M}^{(3)}_{(e)} = \frac{g}{6f_K^2 f_\pi}(q\cdot\varepsilon)[J_0^c(m_{K^+}) - J_0^c(m_{K^0})], \tag{20}$$

$$i\mathcal{M}^{(3)}_{(f)} = -\frac{g(q\cdot\varepsilon)}{2\sqrt{3}f_K^2 f_\eta}\theta_{\eta\pi^0}[J_0^c(m_{K^0}) + J_0^c(m_{K^+})], \tag{21}$$

$$i\mathcal{M}^{(3)}_{(g)} = i\mathcal{M}^{(3)}_{(h)} = i\mathcal{M}^{(3)}_{(i)} = i\mathcal{M}^{(3)}_{(j)} = 0. \tag{22}$$

For the renormalization of the wave functions of the D_s meson,

$$i\mathcal{M}^{(3)}_{(k)} = i\mathcal{M}^{(1)}\delta Z_{D_s}, \tag{23}$$

where

$$\delta Z_{D_s} = Z_{D_s} - 1 = \frac{1}{2}\frac{\partial\Sigma_{D_s}(m_\phi,\omega)}{\partial\omega}\bigg|_{\omega=-\Delta_3}. \tag{24}$$

And for the renormalization of the wave functions of the D_s^* meson,

$$i\mathcal{M}^{(3)}_{(l+m)} = i\mathcal{M}^{(1)}\delta Z_{D_s^*}, \tag{25}$$

where

$$\delta Z_{D_s^*} = Z_{D_s^*} - 1 = -\frac{1}{2}\frac{\partial\Sigma_{D_s^*}(m_\phi,\omega,\delta)}{\partial\omega}\bigg|^{\omega=\Delta_3}_{\delta=0}. \tag{26}$$

In Eqs. (24) and (26), the expressions of Σ_{D_s} and $\Sigma_{D_s^*}$ read

$$\Sigma_{D_s} = (1-d)g^2\left[\frac{2}{f_K^2}J_{22}^a(m_K,\omega) + \frac{2}{3f_\eta^2}J_{22}^a(m_\eta,\omega)\right],$$
$$\Sigma_{D_s^*} = \frac{2g^2}{f_K^2}J_{22}^A(m_K,\omega,\delta) + \frac{2g^2}{3f_\eta^2}J_{22}^A(m_\eta,\omega,\delta), \tag{27}$$

where the functions $F(m,\omega,\delta)$, $J_c^0(m)$, and $J_{22}^a(m,\omega)$ are the loop integrals, which are calculated with the dimensional regularization in d dimensions. Their definitions and expressions are collected in the Appendix. Note that J_{22}^A is defined as

$$J_{22}^A(m,\omega,\delta) = J_{22}^a(m,\omega) + 2J_{22}^a(m,\delta). \tag{28}$$

The parameters $\omega_{1,2,3}$, $\delta_{1,2,3}$, and $\Delta_{1,2,3}$ are given as

$$\omega_1 = E - m_{D^0}, \quad \omega_2 = E - m_{D^-}, \quad \omega_3 = E - m_{D_s}, \tag{29}$$

$$\delta_1 = E - q_0 - m_{D^{0*}}, \quad \delta_2 = E - q_0 - m_{D^{-*}}, \quad \delta_3 = E - q_0 - m_{D_s^*}, \tag{30}$$

$$\Delta_1 = m_{D^{*0}} - m_{D^0}, \quad \Delta_2 = m_{D^{*-}} - m_{D^-}, \quad \Delta_3 = m_{D_s^*} - m_{D_s}, \tag{31}$$

where E is the energy of D_s^*, which equals $m_{D_s^*}$ in the center-of-mass frame of the initial state.

For the $\mathcal{O}(p^3)$ tree diagrams in Fig. 4, their amplitudes read

$$i\mathcal{M}^{(3)}_{\text{tree}} = i\mathcal{M}_{(a1)} + i\mathcal{M}_{(a2)} + i\mathcal{M}_{(b)}, \tag{32}$$

with

$$i\mathcal{M}_{(a1)} = i\mathcal{M}^{(1)}\frac{1}{g\Lambda_\chi^2}[2(b_1-2c_1)m_\eta^2 - (2b_1+d_1)m_\pi^2],$$
$$i\mathcal{M}_{(a2)} = i\mathcal{M}^{(1)}\frac{1}{g\Lambda_\chi^2}[3(b_2-2c_2)m_\eta^2 + 3(b_2+2c_2)m_\pi^2],$$
$$i\mathcal{M}_{(b)} = i\mathcal{M}^{(1)}\frac{1}{g\Lambda_\chi^2}(4c_1-6c_2)(m_\eta^2 - m_\pi^2), \tag{33}$$

where $\mathcal{M}^{(1)}$ is the $\mathcal{O}(p)$ amplitude in Eq. (14). The contribution of the first $\mathcal{O}(p^3)$ tree diagram contains two parts, $i\mathcal{M}_{(a1)}$ and $i\mathcal{M}_{(a2)}$. The second part can be absorbed into the leading order diagram because they have the same Lorentz structure except for a constant factor. We ignore the isospin breaking effect from the decay constants of the light

pseudoscalar mesons when calculating the contribution of the loop diagrams because the isospin breaking effect from the K meson decay constant is about 0.1% [37,49,50].

In addition, we adopt the experimental values for the decay constants of π, K, and η, respectively; they include the corrections from all orders. Thus, our analysis is actually based on the reordered series, which would introduce some minor errors at the order in which we are working. The error originates from higher order contributions, which are marginal and negligible considering the good convergence of the chiral expansion. Therefore, the errors in our latter analysis are mainly given by the $\mathcal{O}(p^3)$ LECs and experimental measurements.

After performing the average over the initial D_s^* polarization, the decay width of $D_s^* \to D_s\pi^0$ can then be written as

$$\Gamma[D_s^* \to D_s\pi^0] = \frac{|\boldsymbol{q}|^3}{24\pi}\frac{m_{D_s}}{m_{D_s^*}}|\mathcal{M}|^2. \tag{34}$$

C. Numerical results

We have derived the analytical expressions of the isospin violating decay $D_s^* \to D_s\pi^0$ with chiral perturbation theory up to $\mathcal{O}(p^3)$. However, the $\mathcal{O}(p^3)$ Lagrangian [see Eq. (10)] contains unknown LECs, which are hard to determine at present. In order to include the effects of the $\mathcal{O}(p^3)$ tree diagrams, we use two different strategies to estimate their contributions.

Strategy A.—We first adopt the nonanalytic dominance approximation [51–53] to estimate the $\mathcal{O}(p^3)$ tree diagram contributions. We know that in chiral perturbation theory, the amplitude of a tree diagram includes the polynomials of m_ϕ^2 and q^2; i.e., it only contains the analytic terms. However, for a loop diagram, its amplitude might contain the polynomials of m_ϕ^2 and q^2 but also have the typical multivalued functions, such as logarithmic and square root terms, which are called nonanalytic terms. The nonanalytic dominance approximation assumes that the analytic parts of $\mathcal{O}(p^3)$ loop diagrams and $\mathcal{O}(p^3)$ tree diagrams are roughly the same. This approximation might be rough, to some extent, but can give us some clear indications about the convergence of the chiral expansion.

The contributions are listed in Table I order by order. The results are given in the cases of $\Delta \neq 0$ and $\Delta = 0$, respectively, where $\Delta = m_{D_{(s)}^*} - m_{D_{(s)}}$. For example, for the case of $\Delta \neq 0$, we keep all the physical mass splittings in the loops, while for the case of $\Delta = 0$, i.e., in the heavy quark limit, we neglect the mass difference of $D_{(s)}^*$ and $D_{(s)}$.

From Table I, we see that the variation of the total decay width of $D_s^* \to D_s\pi^0$ is not obvious, whereas the change of contribution from the $\mathcal{O}(p^3)$ loop diagrams is evident with $\Delta \neq 0$ and $\Delta = 0$. In other words, the heavy quark symmetry breaking effect at the loop level is significant for the charm sectors. This effect has been noted in some previous works [15,54]. Additionally, we give the contributions of each $\mathcal{O}(p^3)$ loop diagram in Table II. We also notice that the convergence of the chiral expansion is very good, even if we work in the SU(3) case. The convergence of the $\Delta = 0$ case is better than that of the $\Delta \neq 0$ case. In Eqs. (35) and (36), we adopt the $\Delta \neq 0$ result to predict the decay width and total width of D_s^*. We then use the largest loop contribution to estimate the $\mathcal{O}(p^3)$ tree-level contribution and treat it as the error of our numerical result. Our calculation yields

$$\Gamma[D_s^* \to D_s\pi^0] = 8.1^{+3.0}_{-2.6}\ \text{eV}. \tag{35}$$

Considering $\Gamma[D_s^* \to D_s\pi^0]/\Gamma[D_s^*] = (5.8 \pm 0.7)\%$, we can estimate the total width of D_s^* with the value in Eq. (35),

$$\Gamma[D_s^*] = 139.0^{+77.9}_{-54.6}\ \text{eV}, \tag{36}$$

which agrees with the one estimated in Ref. [15].

Strategy B.—We consider the naturalness of chiral perturbation theory [55,56]. The amplitude can be expanded generally in a power series of q/Λ_χ as follows,

$$\mathcal{M} = \mathcal{M}^{(0)}\sum_\mu \left(\frac{q}{\Lambda_\chi}\right)^\mu \mathcal{F}(g_i), \tag{37}$$

where $\mathcal{M}^{(0)}$ is the leading order amplitude, μ is the chiral order, and $\mathcal{F}(g_i)$ is a function of LECs. Therefore, in order to keep the convergence of the chiral expansion, a natural assumption requires that the function $\mathcal{F}(g_i)$ should be order one. The above is the naturalness assumption of chiral perturbation theory.

For the $\mathcal{O}(p^3)$ tree diagrams with unknown LECs, except the terms which can be absorbed by the $\mathcal{O}(p^1)$ Lagrangian, we can rewrite the remaining two parts as follows,

TABLE I. The contributions order by order and the decay width of $D_s^* \to D_s\pi^0$ with $\Delta \neq 0$ and $\Delta = 0$, respectively. We give the numerical results of the structure $i\mathcal{M}/(q\cdot\epsilon)$ in units of 10^{-3} GeV^{-1} and the decay width in units of eV.

Mass splitting	$\mathcal{O}(p)$	$\mathcal{O}(p^3)_{\text{loop}}$	$\mathcal{O}(p^3)_{\text{tree}}$	Total	Γ
$\Delta \neq 0$	−69.5	−7.2	±13.1	$-76.7^{+13.1}_{-13.1}$	$8.1^{+3.0}_{-2.6}$ eV
$\Delta = 0$	−69.5	−5.9	…	−75.4	7.8 eV

TABLE II. The contributions of each $\mathcal{O}(p^3)$ loop diagram with $\Delta \neq 0$ and $\Delta = 0$, respectively. We give the numerical results of the structure $i\mathcal{M}/(q\cdot\epsilon)$ in units of 10^{-3} GeV^{-1}.

Mass splitting	a	b	c	d	e	f	k	$l+$m
$\Delta \neq 0$	−1.9	−2.4	7.2	4.6	1.5	−7.2	4.5	−13.4
$\Delta = 0$	0.6	−0.4	−1.3	0.8	1.5	−7.2	−6.0	−10.1

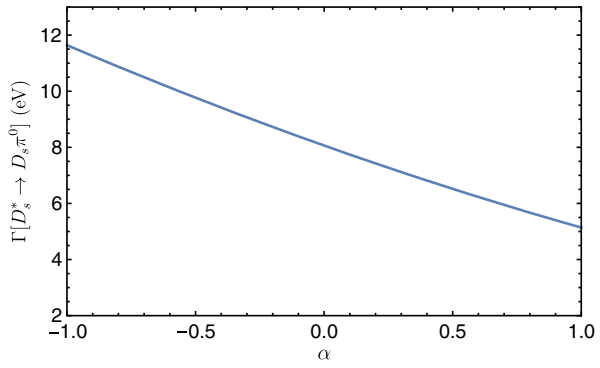

FIG. 5. The change of the decay width of $D_s^* \to D_s\pi^0$ with the parameter α.

$$i\mathcal{M}_{\text{tree}}^{(3)a1} = i\mathcal{M}^{(1)}\frac{1}{(4\pi F_\pi)^2}\alpha\left(-m_\eta^2 - \frac{3}{2}m_\pi^2\right), \quad (38)$$

$$i\mathcal{M}_{\text{tree}}^{(3)b} = i\mathcal{M}^{(1)}\frac{1}{(4\pi F_\pi)^2}\alpha(-m_\eta^2 + m_\pi^2). \quad (39)$$

Here, we replace all of the $\mathcal{O}(p^3)$ LECs as $\alpha g/2$, where g is the LEC of the leading order Lagrangian and the parameter α is an order one number. The effect of the $\mathcal{O}(p^3)$ LECs can be roughly represented by the size of the parameter α. Thus, in order to discuss the contribution of the $\mathcal{O}(p^3)$ tree diagrams in detail, we change the parameter from -1 to 1. The change of the total decay width with the parameter is shown in Fig. 5. When α varies from -1 to 1, the range of $\Gamma[D_s^* \to D_s\pi^0]$ is [5.2, 11.7] eV, which is consistent with the result estimated in strategy A. We can see that the contribution of the $\mathcal{O}(p^3)$ tree diagrams could be quite large. Nominally, the $\mathcal{O}(p^3)$ tree diagrams should be suppressed by the factor $1/(4\pi F_\pi)^2$. But the η meson mass is 547.8 MeV, which makes the correction not as small as one naively guesses. Thus, the $\mathcal{O}(p^3)$ correction is important.

IV. SUMMARY

Heavy quark spin symmetry implies that the mass difference between the vector mesons D^* and pseudoscalar mesons D is small. Their mass splittings lie above the pion mass with 2–3 MeV. Therefore, the lowest D^* mesons only have two main decay modes. One is the pion emission strong decay $D^* \to D\pi$, and the other one is the electromagnetic $D^* \to D\gamma$ decay. Generally, the decay width of the latter one is usually much smaller than the first one due to the strength of the interactions. However, for the charmed strange meson D_s^*, the strong decay mode $D_s^* \to D_s\pi^0$ is much smaller than the electromagnetic one [37] due to the double suppression of the phase space and isospin violation.

In this work, we have systematically calculated the isospin violating decay $D_s^* \to D_s\pi^0$ with heavy meson chiral perturbation theory up to $\mathcal{O}(p^3)$ including the loop diagrams. The analytical expressions are derived up to chiral order $\mathcal{O}(p^3)$. For this process, the $\mathcal{O}(p^2)$ Lagrangian does not exist under the constraint of the parity and Lorentz symmetries. The corrections to the leading order contribution come from the $\mathcal{O}(p^3)$ tree and loop diagrams. The vertices of the $\mathcal{O}(p^3)$ loop diagrams are governed by the leading order Lagrangians. Thus, the numerical result of the loop diagrams only depends on one parameter, g, which has been well determined by experiments and lattice QCD. Our calculation of the leading order amplitude and $\mathcal{O}(p^3)$ loop diagrams shows very good convergence of the chiral expansion. The convergence in the $\Delta = 0$ case is better than that in the $\Delta \neq 0$ one.

The $\mathcal{O}(p^3)$ tree-level amplitudes contain four undetermined LECs. We use two strategies to estimate the uncertainty of the $\mathcal{O}(p^3)$ tree-level contributions. With the nonanalytic dominance approximation, we get $\Gamma[D_s^* \to D_s\pi^0] = 8.1^{+3.0}_{-2.6}$ eV. With the naturalness assumption of chiral perturbation theory, we give a possible range of the isospin violating decay width, [5.2, 11.7] eV. We find that the contribution of the $\mathcal{O}(p^3)$ tree diagrams might be significant compared with the leading order one.

The isospin violating decay plays a very important role in studying the character and structure of the D_s^* meson. We expect that experiments and lattice QCD can provide more results about the decays of the charmed mesons in the future. Our analytical expressions can also be helpful for chiral extrapolation in lattice QCD simulations.

ACKNOWLEDGMENTS

B. Y. is grateful to W. Z. Deng and X. L. Chen for very helpful discussions. This project is supported by the National Natural Science Foundation of China under Grant No. 11975033.

APPENDIX: DEFINITIONS AND EXPRESSIONS OF THE LOOP INTEGRALS

The loop functions used in Eqs. (14)–(33) are defined as follows,

$$F(m_\phi,\omega,\delta) \equiv \frac{1}{d-1}[(m_\phi^2-\delta^2)J_0^a(m_\phi,\delta) - (m_\phi^2-\omega^2) \times J_0^a(m_\phi,\omega) + (\delta-\omega)J_0^c(m_\phi)], \quad (A1)$$

$$J_0^c(m_\phi) \equiv i\int\frac{d^dk\lambda^{4-d}}{(2\pi)^d}\frac{1}{k^2-m_\phi^2+i\epsilon}, \quad (A2)$$

$$J_0^a(m_\phi,\omega) \equiv i\int\frac{d^dk\lambda^{4-d}}{(2\pi)^d}\frac{1}{[k^2-m_\phi^2+i\epsilon][v\cdot k+\omega+i\epsilon]}, \quad (A3)$$

$$i\int\frac{d^dk\lambda^{4-d}}{(2\pi)^d}\frac{k^\mu k^\nu}{[k^2-m_\phi^2+i\epsilon][v\cdot k+\omega+i\epsilon]} \equiv v^\mu v^\nu J_{21}^a(m_\phi,\omega)+g^{\mu\nu}J_{22}^a(m_\phi,\omega). \quad \text{(A4)}$$

The above loop integrals can be calculated with the dimensional regularization in d dimensions. Their expressions read

$$J_0^c(m)=-\frac{m^2}{16\pi^2}\left(L+\ln\frac{\lambda^2}{m^2}\right), \quad \text{(A5)}$$

$$J_{22}^a(m,\omega)=\frac{1}{d-1}[(m^2-\omega^2)J_0^a(m,\omega)+\omega J_0^c(m)]. \quad \text{(A6)}$$

We adopt the $\overline{\text{MS}}$ scheme to renormalize the loop integrals. Here, L is defined as follows,

$$L=\frac{2}{4-d}+\ln 4\pi-\gamma_E+1, \quad \text{(A7)}$$

where $\gamma_E\approx 0.5772$ is the Euler-Mascheroni constant.

$$J_0^a(m,\omega)=\begin{cases}-\frac{\omega}{8\pi^2}(L+\ln\frac{\lambda^2}{m^2}+1)+\frac{1}{4\pi^2}\sqrt{\omega^2-m^2}\,\text{arccosh}(\frac{\omega}{m})-\frac{i}{4\pi}\sqrt{\omega^2-m^2} & (\omega>m)\\ -\frac{\omega}{8\pi^2}(L+\ln\frac{\lambda^2}{m^2}+1)+\frac{1}{4\pi^2}\sqrt{m^2-\omega^2}\arccos(-\frac{\omega}{m}) & (-m<\omega<m)\\ -\frac{\omega}{8\pi^2}(L+\ln\frac{\lambda^2}{m^2}+1)-\frac{1}{4\pi^2}\sqrt{\omega^2-m^2}\,\text{arccosh}(-\frac{\omega}{m}) & (\omega<-m).\end{cases} \quad \text{(A8)}$$

[1] M.-L. Du, M. Albaladejo, P. Fernndez-Soler, F.-K. Guo, C. Hanhart, U.-G. Meiner, J. Nieves, and D.-L. Yao, Phys. Rev. D **98**, 094018 (2018).
[2] X.-Y. Guo, Y. Heo, and M. F. M. Lutz, Phys. Rev. D **98**, 014510 (2018).
[3] Y.-B. Dai, C.-S. Huang, C. Liu, and S.-L. Zhu, Phys. Rev. D **68**, 114011 (2003).
[4] C. B. Lang, L. Leskovec, D. Mohler, S. Prelovsek, and R. M. Woloshyn, Phys. Rev. D **90**, 034510 (2014).
[5] C. Alexandrou, J. Berlin, J. Finkenrath, T. Leontiou, and M. Wagner, Phys. Rev. D **101**, 034502 (2020).
[6] H.-X. Chen, W. Chen, X. Liu, Y.-R. Liu, and S.-L. Zhu, Rep. Prog. Phys. **80**, 076201 (2017).
[7] M. B. Wise, Phys. Rev. D **45**, R2188 (1992).
[8] G. Burdman and J. F. Donoghue, Phys. Lett. B **280**, 287 (1992).
[9] T.-M. Yan, H.-Y. Cheng, C.-Y. Cheung, G.-L. Lin, Y. C. Lin, and H.-L. Yu, Phys. Rev. D **46**, 1148 (1992); **55**, 5851(E) (1997).
[10] H.-Y. Cheng, C.-Y. Cheung, G.-L. Lin, Y. C. Lin, T.-M. Yan, and H.-L. Yu, Phys. Rev. D **47**, 1030 (1993).
[11] P. L. Cho and H. Georgi, Phys. Lett. B **296**, 408 (1992); **300**, 410(E) (1993).
[12] J. F. Amundson, C. G. Boyd, E. E. Jenkins, M. E. Luke, A. V. Manohar, J. L. Rosner, M. J. Savage, and M. B. Wise, Phys. Lett. B **296**, 415 (1992).
[13] R. Casalbuoni, A. Deandrea, N. Di Bartolomeo, R. Gatto, F. Feruglio, and G. Nardulli, Phys. Rep. **281**, 145 (1997).
[14] C.-Y. Cheung and C.-W. Hwang, J. High Energy Phys. 04 (2014) 177.
[15] B. Wang, B. Yang, L. Meng, and S.-L. Zhu, Phys. Rev. D **100**, 016019 (2019).
[16] S. Godfrey and N. Isgur, Phys. Rev. D **32**, 189 (1985).
[17] E. Sucipto and R. L. Thews, Phys. Rev. D **36**, 2074 (1987).
[18] A. N. Kamal and Q. P. Xu, Phys. Lett. B **284**, 421 (1992).
[19] N. Barik and P. C. Dash, Phys. Rev. D **49**, 299 (1994); **53**, 4110(E) (1996).
[20] M. A. Ivanov and Yu. M. Valit, Z. Phys. C **67**, 633 (1995).
[21] W. Jaus, Phys. Rev. D **53**, 1349 (1996); **54**, 5904(E) (1996).
[22] H.-M. Choi, Phys. Rev. D **75**, 073016 (2007).
[23] P. Colangelo, F. De Fazio, and G. Nardulli, Phys. Lett. B **316**, 555 (1993).
[24] T. M. Aliev, E. Iltan, and N. K. Pak, Phys. Lett. B **334**, 169 (1994).
[25] T. M. Aliev, D. A. Demir, E. Iltan, and N. K. Pak, Phys. Rev. D **54**, 857 (1996).
[26] H. G. Dosch and S. Narison, Phys. Lett. B **368**, 163 (1996).
[27] S.-L. Zhu, W.-Y. P. Hwang, and Z.-s. Yang, Mod. Phys. Lett. A **12**, 3027 (1997).
[28] Z.-G. Wang, Eur. Phys. J. C **75**, 427 (2015).
[29] J. L. Goity and W. Roberts, Phys. Rev. D **64**, 094007 (2001).
[30] D. Ebert, R. N. Faustov, and V. O. Galkin, Phys. Lett. B **537**, 241 (2002).
[31] V. Simonis, arXiv:1803.01809.
[32] H.-B. Deng, X.-L. Chen, and W.-Z. Deng, Chin. Phys. C **38**, 013103 (2014).
[33] Y.-L. Luan, X.-L. Chen, and W.-Z. Deng, Chin. Phys. C **39**, 113103 (2015).
[34] G. A. Miller and P. Singer, Phys. Rev. D **37**, 2564 (1988).
[35] A. Deandrea, N. Di Bartolomeo, R. Gatto, G. Nardulli, and A. D. Polosa, Phys. Rev. D **58**, 034004 (1998).
[36] D. Becirevic and B. Haas, Eur. Phys. J. C **71**, 1734 (2011).
[37] M. Tanabashi *et al.* (Particle Data Group), Phys. Rev. D **98**, 030001 (2018).
[38] J. Gronberg *et al.* (CLEO Collaboration), Phys. Rev. Lett. **75**, 3232 (1995).

[39] B. Aubert *et al.* (*BABAR* Collaboration), Phys. Rev. D **72**, 091101 (2005).
[40] P. L. Cho and M. B. Wise, Phys. Rev. D **49**, 6228 (1994).
[41] A. N. Ivanov, arXiv:hep-ph/9805347.
[42] K. Terasaki, arXiv:1511.05249.
[43] H.-Y. Cheng, C.-Y. Cheung, G.-L. Lin, Y. C. Lin, T.-M. Yan, and H.-L. Yu, Phys. Rev. D **49**, 5857 (1994); **55**, 5851(E) (1997).
[44] H.-Y. Cheng, C.-Y. Cheung, G.-L. Lin, Y. C. Lin, T.-M. Yan, and H.-L. Yu, Phys. Rev. D **49**, 2490 (1994).
[45] A. N. Ivanov and N. I. Troitskaya, Phys. Lett. B **345**, 175 (1995).
[46] A. N. Ivanov and N. I. Troitskaya, Phys. Lett. B **394**, 195 (1997).
[47] P. L. Cho, Phys. Lett. B **285**, 145 (1992).
[48] W. Detmold, C. J. D. Lin, and S. Meinel, Phys. Rev. D **85**, 114508 (2012).
[49] V. Cirigliano and H. Neufeld, Phys. Lett. B **700**, 7 (2011).
[50] N. Carrasco *et al.*, Phys. Rev. D **91**, 054507 (2015).
[51] J. Bijnens, G. Colangelo, G. Ecker, J. Gasser, and M. E. Sainio, Phys. Lett. B **374**, 210 (1996).
[52] Z.-W. Liu and S.-L. Zhu, Phys. Rev. D **86**, 034009 (2012); **93**, 019901(E) (2016).
[53] B. Wang, Z.-W. Liu, and X. Liu, Phys. Rev. D **99**, 036007 (2019).
[54] B. Wang, L. Meng, and S.-L. Zhu, J. High Energy Phys. 11 (2019) 108.
[55] E. Epelbaum, H.-W. Hammer, and U.-G. Meissner, Rev. Mod. Phys. **81**, 1773 (2009).
[56] L. Meng and S.-L. Zhu, Phys. Rev. D **100**, 014006 (2019).